Journal of Power Sources 580 (2023) 233437

Contents lists available at ScienceDirect

Journal of Power Sources

journal homepage: www.elsevier.com/locate/jpowsour

Efficient improvement in electrochemical properties of high-voltage Li-rich Mn-based layered oxide cathode by addition of 1,3-divinyltetramethyldisiloxane to electrolyte

Tao Huang, Xiangzhen Zheng, Chunfeng Yan, Ying Pan, Maoxiang Wu *

Key Laboratory of Optoelectronic Materials Chemistry and Physics, Fujian Institute of Research on the Structure of Matter, Chinese Academy of Sciences, Fuzhou, 350002, PR China

HIGHLIGHTS

- DTMS improved cyclic stability of LRM cathode lithium-ion batteries.
- The DTMS-derived layer maintains interface stability.
- DTMS reacts with the HF/F^- from the electrolyte.

ARTICLE INFO

Keywords:
Lithium-ion battery
Li-rich layered oxide cathode
Solid electrolyte interphase film
Interfacial stability
1,3-divinyltetramethyldisiloxane

ABSTRACT

1,3-Divinyltetramethyldisiloxane (DTMS) is a multifunctional additive that is used to improves the cycling stability and capacity retention of Li-rich Mn-based layered oxide cathodes (LRMs). Cycling performance evaluations demonstrate that LRM/Li cells without the additive exhibit lower capacity retention. DTMS can significantly improve the capacity retention of LRM/Li cells from 42.8% to 75% at 0.5C. Theoretical calculations indicate that DTMS is preferentially oxidized on the LRM surface. Physical characterization results reveal that DTMS generates a layer on the LRM surface that is both less resistive and thinner than the LRM by reacting with HF/F^- from the electrolyte. This DTMS-derived layer inhibits adverse reactions between the cathode and electrolyte, thus, effectively maintaining the cathode structure.

1. Introduction

Lithium ion batteries (LIBs) have been used in electric vehicles because of their high energy density, safety, and low price; however, these qualities need to be further enhanced to extend the maximum distance that electric vehicles can travel before needing to be recharged [1–3]. Many novel and advanced types of cathode materials have been explored and had their potentials gauged to meet the requirements of a high cell energy density [4]. Lithium-rich layered oxide (LRM), $xLi_2MnO_3{\cdot}(1\text{-}x)LiMO_2$ (M = Ni, Co, Mn) has attracted considerable attention as the most promising alternative for LIBs, due to its high reversible discharge capacity (over 250 mAh g^{-1}) and high range of operating voltage (3.0–4.8 V) [5–8]. However, its application is limited by the poor cycling and rate performance of LRM, which leads to the destruction of the cathode material structure and an unstable electrode/electrolyte interface [9].

To overcome these problems, several approaches have been explored in the past decade, including doping and coating [10–13]. Recently, a simple and economical strategy has been developed: the formation of a protective interphase on the cathode through the preferential oxidation of additives (<5 wt%) added to the electrolyte. These additives have a higher highest occupied molecular orbital than solvents. This ensures that the electrolyte decomposition products do not react with the protective cathode interphase, resulting in the maintenance of interface stability. A variety of electrolyte additives with different molecular structures have been proposed. Tris(trimethylsilyl)phosphate [14,15] has been used as a film-forming additive on lithium-rich cathode materials to improve the electrochemical performance. Tris(trimethylsilyl) borate forms a modified solid electrolyte interphase (CEI) on the cathode, which reduces the capacity fading of a $Li[Li_{0.2}Mn_{0.54}Ni_{0.13}Co_{0.13}]$

* Corresponding author.
E-mail address: mxwu@fjirsm.ac.cn (M. Wu).

https://doi.org/10.1016/j.jpowsour.2023.233437
Received 28 February 2023; Received in revised form 7 June 2023; Accepted 17 July 2023
Available online 26 July 2023
0378-7753/© 2023 Elsevier B.V. All rights reserved.

O_2/Li cell from 81% to 26% after 200 cycles [16]. Lan et al. reported [17] that the electrode capacity retention in an electrolyte without any additive was 40%, which is much lower than the 72% observed in an electrolyte with bis(trimethylsilyl)carbodiimide. The capacity retention of $Li_{1.2}Mn_{0.54}Ni_{0.13}Co_{0.13}O_2$ cathodes was found to increase in an electrolyte with 1 wt% diphenyl disulfide [18]. After 150 cycles, the capacity fading of $Li_{1.2}Mn_{0.54}Ni_{0.13}Co_{0.13}O_2$ was found to decrease from 27.4% in an electrolyte without any additive to 8.8% an electrolyte with 1% 1,3,6-hexanetricarbonitrile [19]. The cycling stability of $Li_{1.2}Mn_{0.525}Ni_{0.175}Co_{0.1}O_2$ cathodes was improved by using 5 wt% di-(2, 2,2 trifluoroethyl) carbonate in the electrolyte, and as a result, the capacity fading decreased from 30% to 11% after 50 cycles [20]. Cha et al. [21] investigated Li-rich/graphite full cells with 1 wt% lithium difluoro (oxalate)borate (LiDFOB) in 1.3 M $LiPF_6$ containing an EC:EMC:DMC electrolyte at a volume ratio of 3:4:3. LiDFOB optimizes the surface composition of both the graphite anode and Li-rich cathode. A stable CEI film was produced on the $Li[Li_{0.2}Mn_{0.56}Ni_{0.16}Co_{0.08}]O_2$ electrode with the presence of the decomposition products of tri(hexafluoro-iso-propyl) phosphate (HFiP). The capacity loss for a $Li[Li_{0.2}Mn_{0.56}Ni_{0.16}Co_{0.08}]O_2$ electrode in an electrolyte with 1% HFiP after 130 cycles was shown to be reduced from 35.5% to 26.7% [22]. Triphenyl phosphite (TPPi) was found to preferentially oxidize over the solvent at an oxidation potential of 4.2 V (vs. Li/Li^+), and the TPPi-derived layer can effectively inhibit electrolyte decomposition [23]. Tu et al. reported that TEP reacted with active oxygen and formed a protective layer that suppressed electrolyte decomposition and the structural destruction of the LRM [24]. Triethyl borate and tripropyl borate have been reported as electrolyte additives that improve the self-discharge property of LRM cathodes [25].

Some studies have reported that the improvement of the electrochemical behavior of NCM622-based cells and LNMO-based cells are a result of silicon-based electrolyte additives [26–28]. In this paper, 1, 3-divinyltetramethyldisiloxane (DTMS) was used as an additive to enhance the electrochemical properties of a Li-rich layered oxide cathode (LRM). Results showed that 2 vol% DTMS effectivity decreased capacity loss of LRM/Li cell from 57.2% to 25%. The possible mechanism for this was investigated further though electrochemical and physical analyses.

2. Experiment

2.1. Preparation of electrolytes and electrodes

The LRM cathode was composed of 80 wt% LRM (LRM300, Ningbo Li-rich Battery Material Technology Co., Ltd., China), 10 wt% polyvinylidene fluoride (PVDF) binder, and 10 wt% acetylene black in *N*-methyl-2-pyrrolidone. The slurry was coated on Al foil, and then vacuum dried at 100 °C for 12 h. The CR2025-cell was fabricated in an Ar-filled glove box with a Li sheet as the anode and Celgard 2325 as the separator. The base (BE) electrolyte contained 1 M LiPF6 and included EC/EMC/DMC (1:1:1, in weight). DTMS (Aladdin Co., Ltd., China) was then added into the BE electrolyte. Electrolytes with 2 vol% DTMS were used (Supplementary Material. 1).

A total of 1000 ppm of hydrofluoric acid (HF) was then added into the BE and BE+2 vol%DTMS electrolytes to prepare HF-containing electrolytes using a 40 wt% HF aqueous solution [25]. All electrolytes were prepared in an Ar-filled glove box.

2.2. Electrochemical testing

The charge–discharge performance of the cells was evaluated using a computer-controlled test system (CT2001A, China). The LRM/Li cells were pre-cycled in the following schedule: 0.1C (1C = 300 mA g^{-1}) for three cycles and 0.2C for three cycles at 25 °C between 2.8 and 4.8 V. The LRM/Li cells were then operated for 100 cycles at 0.5C to analyze the cycling performance. The rate capability of the cells was evaluated at a 0.5-1-2-3-5C charge/discharge current. The electrochemical impedance spectroscopy (EIS) was employed in the frequency range of 10^5 to 0.1 Hz with an amplitude of 5 mV, using a frequency response analyzer (VSP, Bio-logic).

Table 1
Calculated Eox (V vs. Li^+/Li) of EC, DMC, EMC, and DTMS.

	Eox/V
EC	7.11
DMC	7.00
EMC	6.99
DTMS	5.58

2.3. Physical characterization

To understand the influence of DTMS on the cycling performance of LRM/Li cells, scanning electron microscopy (SEM; S-4800, Hitachi), transmission electron microscopy (TEM; JEM-2010, JELO), XRD analysis (XRD; Bruker D8 ADVANCE) using Cu Ka radiation, X-ray photoelectron spectroscopy (XPS; ESCALAB 250Xi), and ^{19}F nuclear magnetic resonance (^{19}F NMR; AVANCE III 400 MHz) analyses were carried out. The cycled electrodes (LRM and Li) were disassembled, rinsed with dimethyl carbonate solvent, and dried under vacuum.

2.4. Calculations

The Gaussian 09 software package was used for theoretical calculations. The equilibrium structures were determined using the B3LYP/6-311G(d,p) level [28]. The oxidation potential (E_{ox}) was obtained as follows[28]:

$$E_{ox}\ (Li^+/Li) = [G(M^+) - G(M)]/F - 1.4\ V$$

3. Results and discussion

3.1. Oxidative stability of DTMS

The as-calculated oxidation potential and Li^+ binding affinity (E_b) are often used to forecast the oxidation tendency of an additive on the cathode surface [29,30]. The film-forming electrolyte additives have a lower oxidation potential than the electrolyte solvents. Therefore, the additives dominate the composition of the CEI film on the cathode. Furthermore, a low value of Li^+ E_b is suitable for the enrichment of the additive on the cathode surface [29]. The calculated E_{ox} values of the solvents and DTMS are listed in Table 1. As per the theoretical calculation results, DTMS (5.58 V) has a lower E_{ox} than EC (7.11 V), DMC (7.00 V), and EMC (6.99 V), indicating that DTMS has a lower oxidation stability than the electrolyte solvents. The optimized structures and solvent-Li^+ and DTMS-Li^+ E_b values are seen in Fig. 1. The E_b value of DTMS is lower than those of solvents. This indicates that the interaction between DTMS and Li^+ is weaker, so DTMS can easily accumulate at the cathode surface. DTMS may thus form a protective film at the positive electrode, as per the theoretical calculation results.

3.2. Impact of DTMS at electrochemical perform

Supplementary Material. 2 shows the charge–discharge curve performance of LRM/Li cells with and without 2 vol% DTMS electrolytes during the first pre-cycle process. It can be found that the cells in the 2 vol% DTMS-containing electrolyte have a large charge capacity of 321.2 mAh g^{-1} and that they delivered a lower coulombic efficiency (92.5%) than the cells in the BE electrolyte (97.2%). This may be due to DTMS oxidation occurring prior to that of electrolyte solvents. Fig. 2 presents the comparison of the cycling performance of LRM/Li cells in the

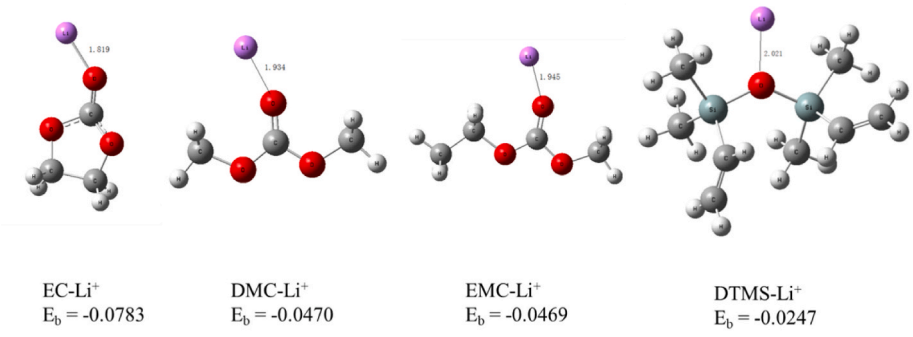

Fig. 1. Optimized structures and E_b values of solvents-Li^+ and DTMS-Li^+.

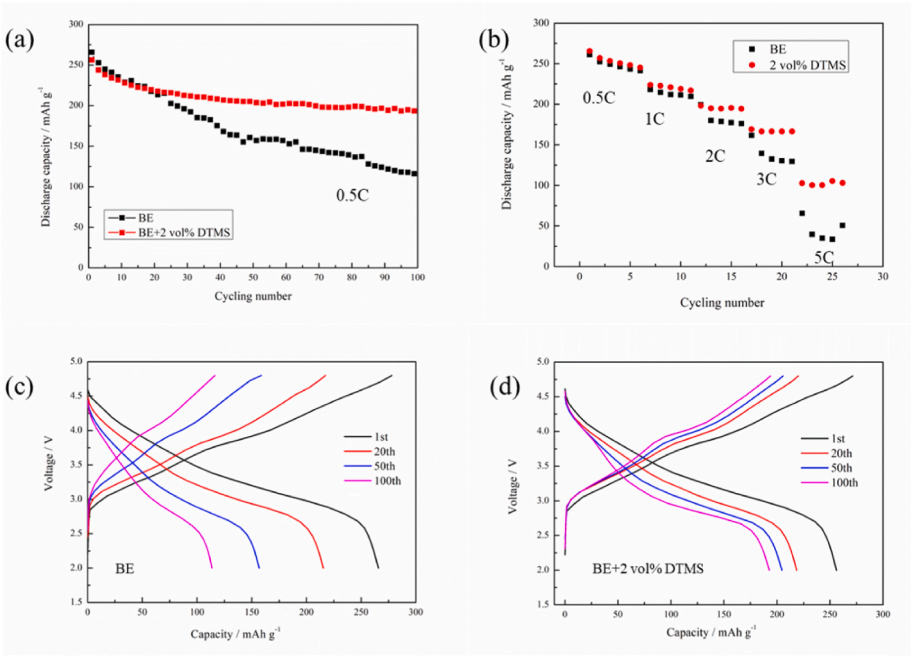

Fig. 2. (a) Cycling performance and (b) rate capability of LRM/Li cell. (c) (d) 1st, 20th, 50th, and 100th charge–discharge curves of LRM/Li cell during cycling.

different electrolytes. The LRM/Li cells with 2 vol% DTMS showed great cycling stability. The discharge capacity of LRM/Li cells in the BE electrolyte decreased from 262.3 to 57.7 mAh g^{-1} after 100 cycles (57.2% capacity loss). However, in the 2 vol% DTMS-containing electrolyte, the discharge capacity decreased from 256.2 to 192.7 mAh g^{-1} (25% capacity loss). To estimate whether the Li/Li-rich cells with the DTMS-containing electrolyte are capable of fast charge transport, the rate capability of LRM/Li cells was evaluated. The Li/Li-rich cells with 2 vol% DTMS delivered a higher discharge capacity of 100 mAh g^{-1} at 5C. In contrast, the LRM/Li cells with the BE electrolyte exhibited substantial capacity loss. The 1st, 20th, 50th, and 100th charge–discharge curves of the LRM/Li cell during cycling are presented in Fig. 2c and d. An obvious decrease in the discharge capacity and voltage platform can be seen for the cell without additives during cycling, which may indicate increased interfacial instability. The charge and discharge capacities of LRM/Li cells in DTMS-containing electrolyte remained at a desirable level.

EIS was carried out on LRM/Li cells after pre-cycling and cycling with the BE and 2 vol% DTMS-containing electrolytes, as shown in Fig. 3. The results can be divided into two parts: a depressed semicircle followed by a slanting line. The depressed semicircle contains two parts: the surface-film resistance (Rf) and the charge-transfer resistance (Rct) between the electrode and electrolyte. [24] The values in Fig. 3c reveal that the cell with the BE electrolyte shows a greater numerical variation in Rf and Rct compared with the cells with the DTMS-containing electrolyte. The electrolyte decomposition substantially deteriorates the properties of the interface between the LRM and BE electrolyte and thereby reduces the cycling performance.

The surface morphologies of the cathodes in the BE and DTMS-containing electrolytes were analyzed after cycling by SEM and TEM (Fig. 4). As shown in Fig. 4a, the cathode surface in the BE electrolyte was covered with a thick and uneven layer. The thickness is approximately 10–15 nm. In contrast, the thickness of the cathode surface in the DTMS-containing electrolytes is only 2–4 nm (Fig. 4b). After cycling, serious structure damage was found for the LRM particles in the BE electrolytes (Fig. 4c). These changes in surface morphology are most likely due to the HF continuous corrosion. The microstructure of the LRM particles in the DTMS-containing electrolytes was well maintained, as shown in Fig. 4d. It could be assumed the CEI layer was created by DTMS inhibiting HF corrosion on the cathode surface.

Fig. 5a depicts the obtained XPS of LRM cells with BE and DMSE-containing electrolytes after cycling. The C 1s peaks at 290.3 and 285.4 eV correspond to PVDF [19,25], and the peak at 284.6 eV is assigned to acetylene black [17]. Furthermore, the peak intensities of the PVDF and acetylene black of the LRM electrode in the BE electrolyte after cycling were higher than those in DTMS-containing electrolytes, which indicates that a thinner CEI film was formed with DTMS. The peaks corresponding to electrolyte decomposition products [19,25]

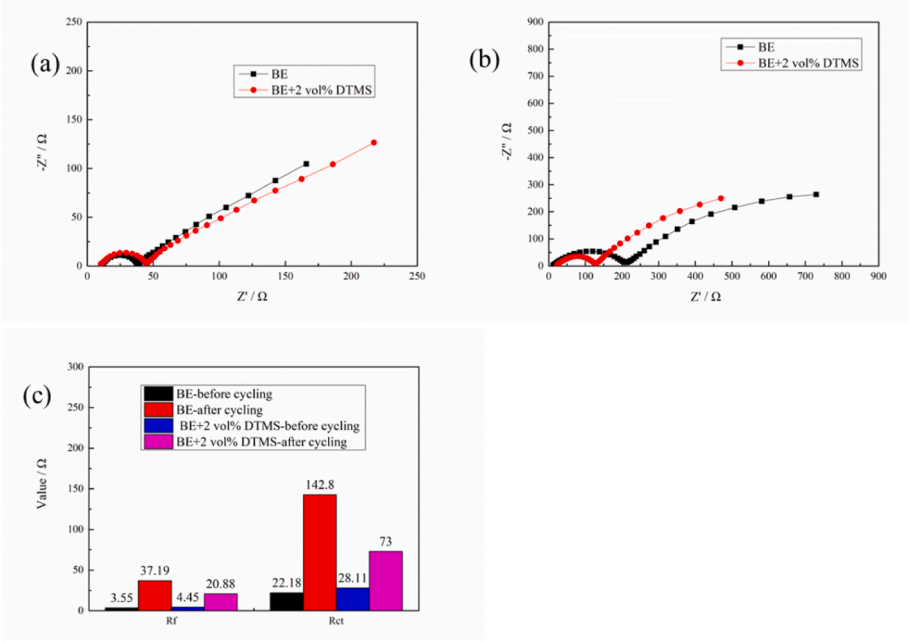

Fig. 3. EIS results of LRM/Li cell in BE and 2 vol% DTMS electrolyte after (a) pre-cycling and (b) cycling. (c) Values of R_f and R_{ct}.

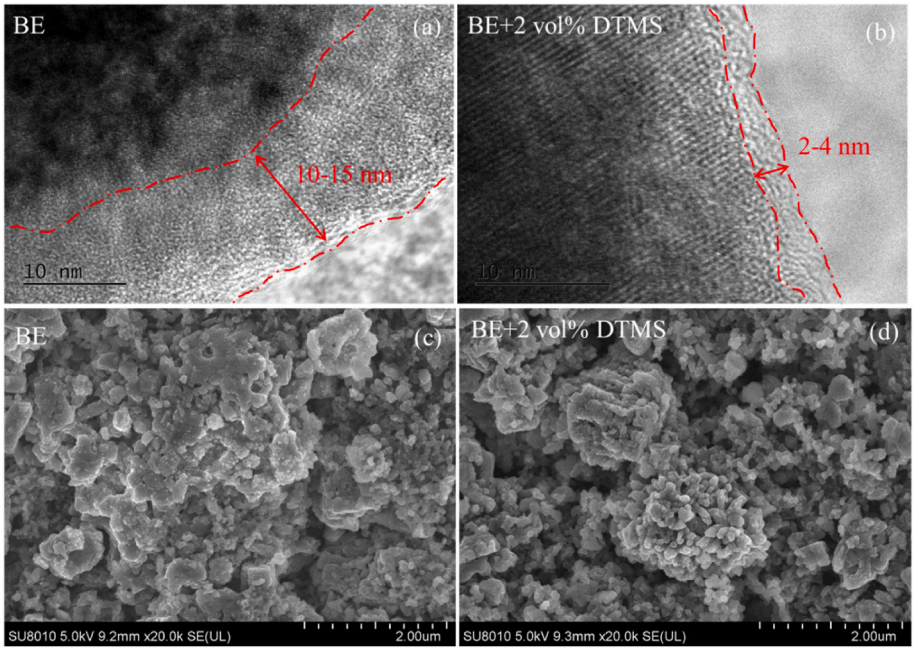

Fig. 4. TEM and SEM images of LRM cathodes after cycling (a), (c) with BE and (b), (d) 2 vol% DTMS electrolyte.

($ROCO_2Li$, ROLi, and Li_2CO_3) at 286 and 288.8 eV were observed. The peak intensities for the electrolyte with DTMS were lower than those for the BE electrolyte. The same result can be observed in O 1s spectra. The peak intensities corresponding to C═O (531.9 eV) [17,19], C–O (533.4 eV)[25], and Li_2CO_3 (531.2 eV) [19] for the electrolyte with DTMS were lower. The F 1s peaks at 684.5 and 685.8 eV were assigned to LiF and Me–F [19], respectively. The peak at 56 eV [31] corresponds to LiF in the Li 1s spectra. For the BE electrolyte, the peak intensities of LiF and Me–F are higher in the F 1s spectra. The peaks at 686.9 eV [19] for Li_xPF_y and $Li_xPO_yF_z$ in the BE electrolyte are higher than those in the DTMS-containing electrolyte in the F 1s spectra, which may be due to the $LiPF_6$ decomposition. This is in accordance with the P 1s spectra for the peaks of LixPFy (136.5 eV) and LixPOyFz (133.8 eV) [23]. In conclusion, the peak intensities for the electrolyte decomposition products on the cathode in the DTMS-containing electrolyte were weaker, confirming that the electrolyte decomposition could be inhibited by DTMS. The existence of Si (Si 2p spectrum) indicates that the film on the cathode is formed from the oxidation of DTMS.

The XRD results for the cathodes before and after cycling with the BE and 2% DTMS-containing electrolytes are shown in Fig. 5b: the XRD peak intensity of the cathode in the BE electrolyte reduces drastically after cycling. The peak (003) broadens and shifts slightly to a higher angle [19], indicating severe structural damage on the LRM electrode in the BE electrolyte. However, after cycling, the LRM electrode with the 2% DTMS-containing electrolyte exhibits almost the same diffraction pattern as that before cycling, indicating that the crystal structure of the

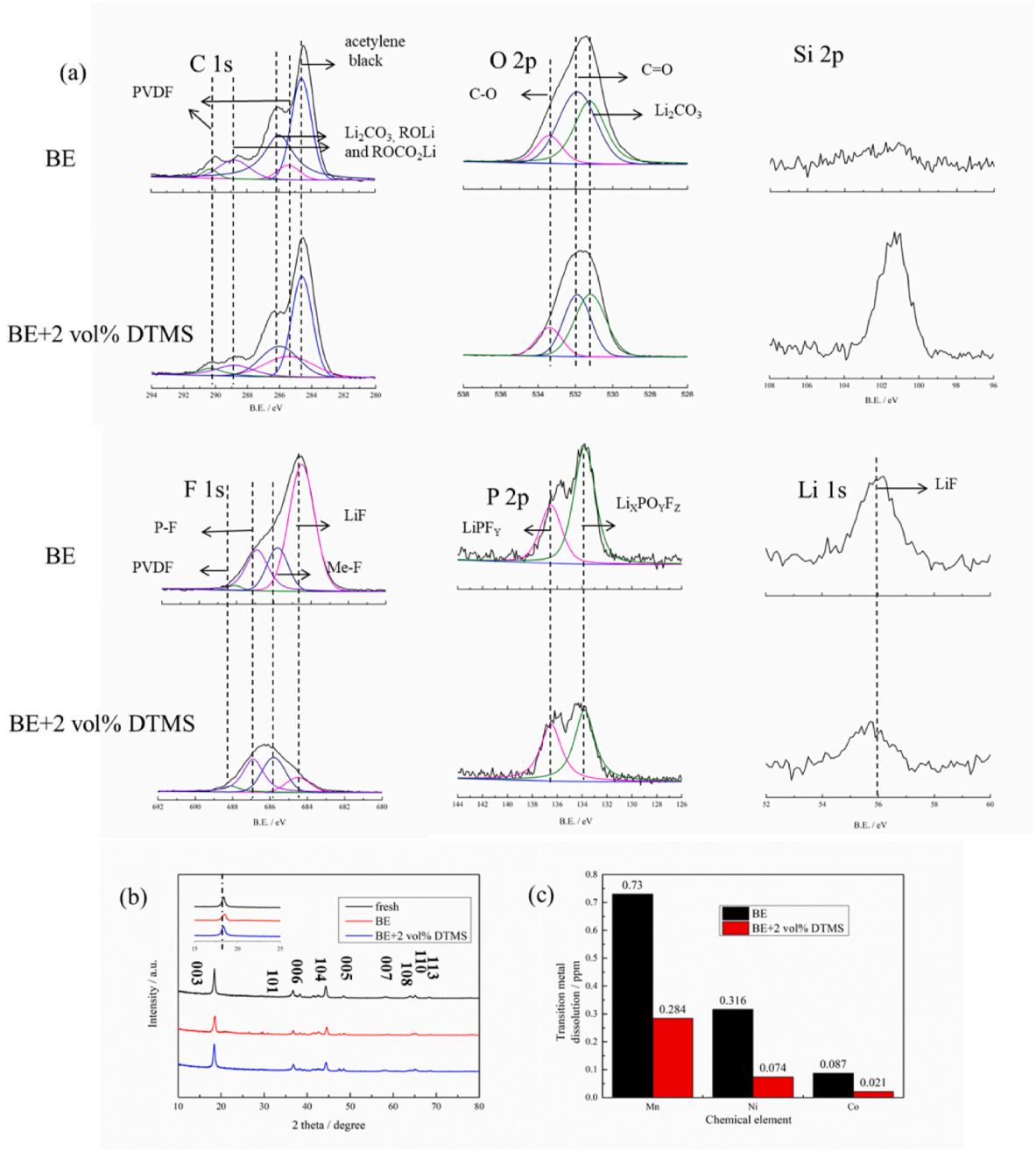

Fig. 5. (a)XPS spectra of LRM cathodes after cycling with BE and 2 vol% DTMS electrolytes. (b) XRD patterns of LRM cathodes and (c) dissolution of transition metal on Li electrode taken from cell after cycling.

cathode was well maintained in DTMS-containing electrolyte. This further confirms that the DTMS is beneficial for maintaining structure stability during cycling. As shown in Fig. 5c, the Mn, Ni, and Co contents were 0.284, 0.074, and 0.021 ppm, respectively, for the electrolyte without an additive, and 0.73, 0.316, and 0.087 ppm, respectively, for the electrolyte with DTMS. Thus, the XRD and ICP-MS results show that the dissolution of transition metals was suppressed by the protective CEI formed via DTMS oxidation.

3.3. Interaction of DTMS with HF/F^-

To study the interaction of DTMS with HF/F^-, the cycling performance of the coin cell in the BE+1000 ppm HF electrolyte and the 2 vol % DTMS-containing+1000 ppm HF electrolyte was analyzed (Fig. 6a). A significant capacity loss was observed after 40 cycles in the case of the BE+1000 ppm HF electrolyte: from 246.4 to 60.3 mAh g^{-1}. However, the discharge capacity in the 2 vol% DTMS-containing+1000 ppm HF electrolyte changed from 240.3 to 190.6 mAh g^{-1}. DTMS can effectively suppress the damage to the cathode by HF and improve battery cycle stability. Fig. 6b and c shows the F 1s XPS spectra of the LRM electrodes in the BE+1000 ppm HF and 2 vol% DTMS+1000 ppm HF electrolyte. The LiF and Me–F peak intensities are much higher in the BE+1000 ppm HF electrolyte than in the 2 vol% DTMS-containing+1000 ppm HF electrolyte. The addition of DMTS could inhibit the fluoride formation.

NMR spectra are used for analyzing the composition changes after storage for 24 h in the electrolyte upon the addition of HF [32] (Fig. 7). A pair of peaks at −75 ppm can be found for all electrolytes, which are assigned to PF_6^- [25]. Unlike the BE (Fig. 7a) and DTMS-containing electrolytes (Fig. 7b), the BE+1000 ppm HF electrolyte shows three additional peaks (Fig. 7c). The pair of weak peaks at −85 ppm is

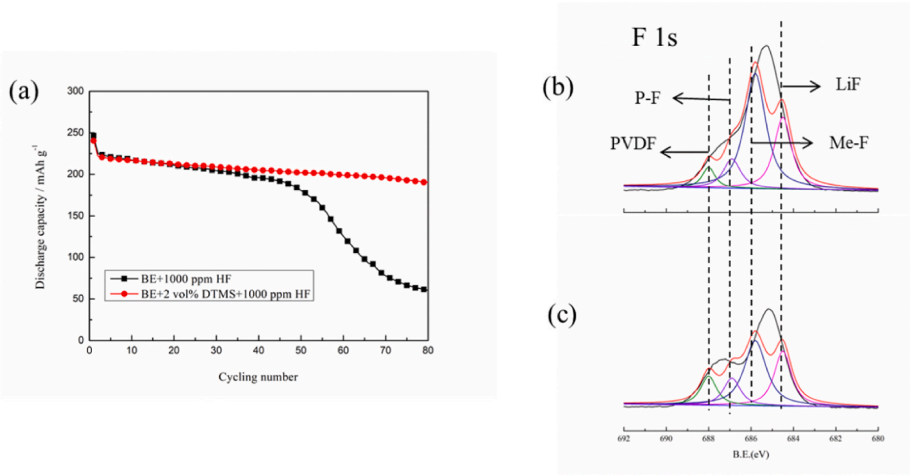

Fig. 6. (a) Discharge profiles of cell during cycling with BE+1000 ppm HF and 2 vol% DTMS-containing+1000 ppm HF; F 1s XPS spectra of LRM cathodes after cycling with (b) BE+1000 ppm HF and (c) 2 vol% DTMS-containing+1000 ppm HF electrolyte.

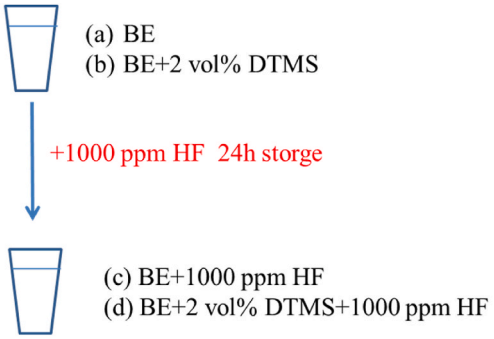

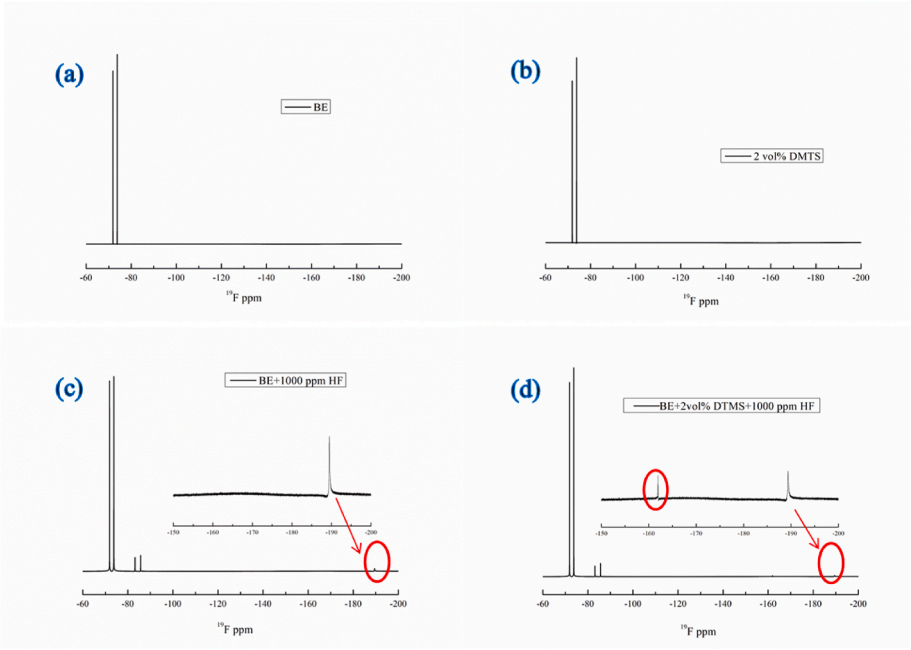

Fig. 7. ^{19}F NMR spectra of BE and DTMS-containing electrolytes before (a and b) and after (c and d) 1000 ppm HF was added.

assigned to $PO_2F_2^-$ formed from the partial hydrolysis of $LiPF_6$ [25], and the peak at 190 ppm corresponds to HF. However, the HF peak intensity for the 2 vol% DTMS-containing+1000 ppm HF electrolyte is lower than that for the BE+1000 ppm HF electrolyte (Fig. 7c and d). In addition, a new small peak at −162 ppm corresponding to the BE+2 vol%DTMS containing 1000 ppm of the HF electrolyte is shown in Fig. 7d, which can be attributed to the reaction between DTMS and HF/F^-.Supplementary Material 3 presents the ^{19}F NMR spectra of the DTMS-containing

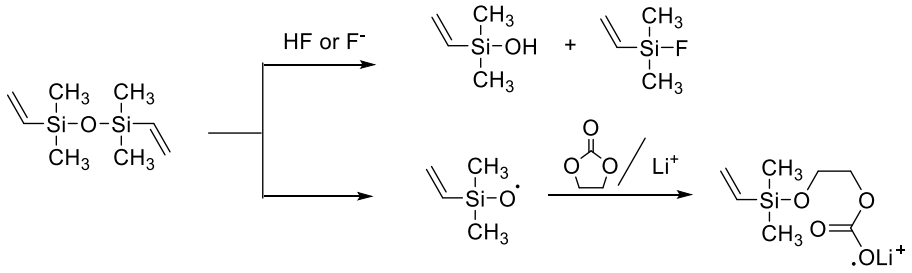

Fig. 8. Possible mechanism of DTMS.

electrolytes collected from the LRM/Li cells after evaluating their cycling performance. In them, the peak at −162 ppm corresponding to the products of the reaction of DTMS with HF/F^- disappears. Combined with the Si 2p XPS results, this demonstrates that DTMS is involved in film formation on the cathode.

The possible DTMS reaction on the interface of the cathode is shown in Fig. 8. We hypothesize that the Si–O bond can react with HF, Lewis acids, and EC [28,33].

4. Conclusions

In conclusion, the cycling performance of the LRM cathode can be greatly improved by adding DTMS. The capacity loss decreased from 57.2% to 25% at 0.5C after 100 cycles. Experimental results show that DTMS is preferentially oxidized on the LRM cathode surface to form a more stable CEI layer with Si–O and Si–F bonds, and that it also reacts with the HF/F^- from the electrolyte, meaning that it is effective for suppressing metal dissolution and enhancing the stability between the electrolyte and cathode.

CRediT authorship contribution statement

Tao Huang: Investigation, Methodology, Writing – original draft. **Xiangzhen Zheng:** Investigation. **Chunfeng Yan:** Validation. **Ying Pan:** Software. **Maoxiang Wu:** Conceptualization, Writing – review & editing.

Declaration of competing interest

The authors declare no competing financial interest.

Data availability

Data will be made available on request.

Acknowledgement

This work was supported by the Science and Technology Planning Project of Fujian Province (Grant No. 2022H0038, 2020H0037, 2022T3001).

Appendix A. Supplementary data

Supplementary data to this article can be found online at https://doi.org/10.1016/j.jpowsour.2023.233437.

References

[1] M. Hu, X. Pang, Z. Zhou, Recent progress in high-voltage lithium ion batteries, J. Power Sources 68 (1997) 604–608, https://doi.org/10.1016/j.jpowsour.2013.03.024.
[2] Q. Zhong, A. Bonakclarpour, M. Zhang, Y. Gao, J.R. Da, Synthesis and electrochemistry of $LiNiMn_{2-x}O_4$, J. Electrochem. Soc. 144 (1997) 205–213, https://doi.org/10.1021/ja3091438.
[3] F. Zhou, X. Zhao, A. Bommel, X. Xia, J.R. Dahn, Comparison of Li$\{Li_1O_9Ni_1O_3Mn_5O_9\}O_2$, Li$\{Li_1O_5Ni_1O_5Mn_3O_5\}O_2$, $LiNi_{0.5}Mn_{1.5}O_4$, and $LiNi_2O_3Mn_1O_3O_2$ as high voltage positive electrode materials, J. Electrochem. Soc. 158 (2011) A187–A191, https://doi.org/10.1039/c1ee01598b.
[4] L. Yang, B. Ravdel, B.L. Lucht, Electrolyte reactions with the surface of high voltage $LiNi_{0.5}Mn_{1.5}O_4$ cathodes for lithium-ion batteries, J. Electrochem. Soc. 13 (2010) A95–A97, https://doi.org/10.1039/c0jm04225k.
[5] K. Xu, A. Cresce, Interfacing electrolytes with electrodes in Li ion batteries, J. Mater. Chem. 21 (2011) 9849–9864, https://doi.org/10.1021/ja108588y.
[6] J. Liu, A. Manthiram, Kinetics study of the 5 V spinel cathode $LiMn_{1.5}Ni_{0.5}O_4$ before and after surface modifications, J. Electrochem. Soc. 156 (2009) A833–A838, https://doi.org/10.1021/cm801245r.
[7] L. Yang, M. Takahashi, B. Wang, A study on capacity fading of lithium-ion battery with manganese spinel positive electrode during cycling, Electrochim. Acta 51 (2006) 3228–3234, https://doi.org/10.1039/c4ra12454e.
[8] D.P. Abraham, T. Spila, M. Furczon, E. Sammann, Evidence of transition-metal accumulation on aged graphite anodes by SIMS, Electrochem. Solid State Lett. 12 (2008) A226–A228, https://doi.org/10.1149/2.0111514jes.
[9] Y. Zhu, X. Luo, M. Xu, L. Zhang, L. Yu, W. Fan, W. Li, Failure mechanism of layered lithium-rich oxide/graphite cell and its solution by using electrolyte additive, J. Power Sources 317 (2016) 65–73, https://doi.org/10.1016/j.jpowsour.2016.03.090.
[10] H. Liu, C. Du, G. Yin, B. Song, P. Zuo, X. Cheng, Y. Ma, Y. Gao, An Li-rich oxide cathode material with mosaic spinel grain and a surface coating for high performance Li-ion batteries, J. Mater. Chem. A 2 (2014) 15640–15646, https://doi.org/10.1039/c4ta02947j.
[11] D. Xie, G. Li, Q. Li, C. Fu, J. Fan, L. Li, Improved cycling stability of cobalt-free Li-rich oxides with a stable interface by dual doping, Electrochim. Acta 196 (2016) 505–516, https://doi.org/10.1016/j.electacta.2016.02.210.
[12] L. Li, B.H. Song, Y.L. Chang, H. Xia, J.R. Yang, K.S. Lee, L. Lu, Retarded phase transition by fluorine doping in Li-rich layered $Li_{1.2}Mn_{0.54}Ni_{0.13}Co_{0.13}O_2$ cathode, Mater. J. Power Sources 283 (2015) 162–170, https://doi.org/10.1016/j.jpowsour.2015.02.085, 283.
[13] H. Liu, C. Chen, C. Du, X. He, G. Yin, B. Song, P. Zuo, X. Cheng, Y. Ma, Y. Gao, Lithium-rich $Li_{1.2}Ni_{0.13}Co_{0.13}Mn_{0.54}O_2$ oxide coated by Li_3PO_4 and carbon nanocomposite layers as high performance cathode materials for lithium ion batteries, J. Mater. Chem. A 3 (2015) 2634–2641, https://doi.org/10.1039/c4ta04823g.
[14] J. Han, S. Lee, J. Lee, J. Kim, K. Lee, N. Choi, Tunable and robust phosphite-derived surface film to protect lithium-rich cathodes in lithium-ion batteries, ACS Appl. Mater. Interfaces 7 (2015) 8319–8329, https://doi.org/10.1021/acsami.5b01770.
[15] J. Zhang, J. Wang, J. Yang, Y. NuLi, Artificial interface deriving from Sacrificial Tris(trimethylsilyl)phosphate additive for lithium rich cathode materials, Electrochim. Acta 117 (2014) 99–104, https://doi.org/10.1016/j.electacta.2013.11.024.
[16] J. Li, L. Xing, R. Zhang, M. Chen, Z. Wang, M. Xu, W. Li, Tris(trimethylsilyl)borate as an electrolyte additive for improving interfacial stability of high voltage layered lithium-rich oxide cathode/carbonate-based electrolyte, J. Power Sources 285 (2015) 360–366, https://doi.org/10.1016/j.jpowsour.2015.03.113.
[17] J. Lan, Q. Zheng, H. Zhou, J. Li, L. Xing, K. Xu, W. Fan, L. Yu, W. Li, Stabilizing a high-voltage lithium-rich layered oxide cathode with a novel electrolyte additive, ACS Appl. Mater. Interfaces 11 (2019) 28841–28850, https://doi.org/10.1021/acsami.9b07441.
[18] X. Zuo, M. Zhao, X. Ma, X. Xiao, J. Liu, J. Nan, Effect of diphenyl disulfide as an additive on the electrochemical performance of $Li_{1.2}Mn_{0.54}Ni_{0.13}Co_{0.13}O_2$/graphite batteries at elevated temperature, Electrochim. Acta 245 (2017) 245 705–714, https://doi.org/10.1016/j.electacta.2017.05.155.
[19] L. Wang, Y. Ma, Q. Li, Z. Zhou, X. Cheng, P. Zuo, C. Du, Y. Gao, G. Yin, 1,3,6-hexanetricarbonitrile as electrolyte additive for enhancing electrochemical performance of high voltage Li-rich layered oxide cathode, J. Power Sources 316 (2017) 227–236, https://doi.org/10.1016/j.jpowsour.2017.06.075.
[20] H. Pham, K. Nam, E. Hwang, Y. Kwon, H. Jung, S. Song, Performance Enhancement of 4.8 V $Li_{1.2}Mn_{0.525}Ni_{0.175}Co_{0.1}O_2$ battery cathode using Fluorinated linear carbonate as a high-voltage additive, J. Electrochem. Soc. 161 (2014) A2002–A2011, https://doi.org/10.1149/2.1141412jes.
[21] J. Cha, J. Han, J. Hwang, J. Cho, N. Choi, Mechanisms for electrochemical performance enhancement by the salt-type electrolyte additive, lithium difluoro (oxalato)borate, in high-voltage lithium-ion batteries, J. Power Sources 357 (2017) 97–106, https://doi.org/10.1016/j.jpowsour.2017.04.094.

[22] S. Tan, Z. Zhang, Y. Li, Y. Li, J. Zheng, Z. Zhou, Y. Yang, Tris(hexafluoro-isopropyl)phosphate as an CEI-forming additive on improving the electrochemical performance of the Li[$Li_{0.2}Mn_{0.56}Ni_{0.16}Co_{0.08}$]$O_2$ cathode, Mater. J. Electrochem. Soc. 160 (2013) A285–A292, https://doi.org/10.1149/2.066302jes.
[23] Z. Zhou, Y. Ma, L. Wang, P. Zuo, X. Cheng, C. Du, G. Yin, Y. Gao, Triphenyl phosphite as an electrolyte additive to improve the cyclic stability of lithium-rich layered oxide cathode for lithium-ion batteries, Electrochim. Acta 216 (2016) 44–50, https://doi.org/10.1016/j.electacta.2016.09.008.
[24] W. Tu, P. Xia, X. Zheng, C. Ye, M. Xu, W. Li, Insight into the interaction between layered lithium-rich oxide and additive-containing electrolyte, J. Power Sources 341 (2017) 348–356, https://doi.org/10.1016/j.jpowsour.2016.12.012.
[25] J. Li, Z. Wang, Triethyl borate and tripropyl borate as electrolyte additives for 4.8 V high voltage layered lithium-rich oxide cathode with enhanced self-discharge suppression performance: a comparative study, J. Power Sources 450 (2020) 227648–227658, https://doi.org/10.1016/j.jpowsour.2019.227648.
[26] S. Wang, S. Chen, W. Gao, L. Liua, S. Zhang, A new additive 3-isocyanatopropyl-triethoxysilane to improve electrochemical performance of Li/NCM622 half-cell at high voltage, J. Power Sources 423 (2019) 90–97, https://doi.org/10.1016/j.jpowsour.2019.03.046.
[27] T.J. Lee, J. Soon, S. Chae, J.H. Ryu, S.M. Oh, A bifunctional electrolyte additive for high-voltage $LiNi_{0.5}Mn_{1.5}O_4$ positive electrodes, ACS Appl. Mater. Interfaces 11 (2019) 11306–11316, https://doi.org/10.1021/acsami.8b19009.
[28] T. Huang, Y. Pan, C. Yan, M. Wu, Electrochemical property enhancement of $LiNi_{0.5}Mn_{1.5}O_4$ cathodes at high temperatures using 1,1,3,3-tetramethyldisiloxane, ACS Appl. Mater. Interfaces 13 (2021) 48881–48888, https://doi.org/10.1021/acsami.1c15137.
[29] J. Chen, H. Zhang, M. Wang, J. Liu, C. Li, P. Zhang, Improving the electrochemical performance of high voltage spinel cathode at elevated temperature by a novel electrolyte additive, J. Power Sources 303 (2016) 41–48, https://doi.org/10.1016/j.jpowsour.2015.10.088.
[30] L. Xing, C. Wang, M. Xu, W. Li, Z. Cai, Theoretical study on reduction mechanism of 1,3-benzodioxol-2-one for the formation of solid electrolyte interface on anode of lithium ion battery, J. Power Sources 189 (2009) 689–692, https://doi.org/10.1016/j.jpowsour.2008.08.076.
[31] Y. Zhu, X. Luo, H. Zhi, Y. Liao, L. Xing, M. Xu, X. Liu, K. Xu, W. Li, Diethyl (thiophen-2-ylmethyl)phosphonate: a novel multifunctional electrolyte additive for high voltage batteries, J. Mater. Chem. A 6 (2018) 10990–11004, https://doi.org/10.1039/c8ta01236a.
[32] Y. Zhu, X. Luo, H. Zhi, Y. Liao, L. Xing, M. Xu, X. Liu, K. Xu, W. Li, Diethyl (thiophen-2-ylmethyl)phosphonate: a novel multifunctional electrolyte additive for high voltage batteries, J. Mater. Chem. A 6 (2018) 10990–11004, https://doi.org/10.1016/j.jpowsour.2019.227366.
[33] H. Wang, D. Sun, X. Li, W. Ge, B. Deng, M. Qu, G. Peng, Alternative multifunctional cyclic organosilicon as an efficient electrolyte additive for high performance lithium-ion batteries, Electrochim. Acta 254 (2017) 112–122, https://doi.org/10.1016/j.electacta.2017.09.111.